Research paper

The Holocene
1–12

Reprints and permissions:
sagepub.co.uk/journalsPermissions.nav
DOI: 10.1177/0959683615574583
hol.sagepub.com
SAGE

A multi-proxy record of hydroclimate, vegetation, fire, and post-settlement impacts for a subalpine plateau, central Rocky Mountains, U.S.A

Lesleigh Anderson,[1] Andrea Brunelle[2] and Robert S Thompson[1]

Abstract
Apparent changes in vegetation distribution, fire, and other disturbance regimes throughout western North America have prompted investigations of the relative importance of human activities and climate change as potential causal mechanisms. Assessing the effects of Euro-American settlement is difficult because climate changes occur on multi-decadal to centennial time scales and require longer time perspectives than historic observations can provide. Here, we report vegetation and environmental changes over the past ~13,000 years as recorded in a sediment record from Bison Lake, a subalpine lake on a high plateau in northwestern Colorado. Results are based on multiple independent proxies, which include pollen, charcoal, and elemental geochemistry, and are compared with previously reported interpretations of hydroclimatic changes from oxygen isotope ratios. The pollen data indicate a slowly changing vegetation sequence from sagebrush steppe during the late glacial to coniferous forest through the late Holocene. The most dramatic vegetation changes of the Holocene occurred during the 'Medieval Climate Anomaly' (MCA) and 'Little Ice Age' (LIA) with rapid replacement of conifer forest by grassland followed by an equally rapid return to conifer forest. Late Holocene vegetation responses are mirrored by changes in fire, lake biological productivity, and watershed erosion. These combined records indicate that subsequent disturbance related to Euro-American settlement, although perhaps significant, had acted upon a landscape that was already responding to MCA-LIA hydroclimatic change. Results document both rapid and long-term subalpine grassland ecosystem dynamics driven by agents of change that can be anticipated in the future and simulated by ecosystem models.

Keywords
Bison Lake, charcoal, Colorado, grasslands, pollen, subalpine, X-ray fluorescence

Received 16 July 2014; revised manuscript accepted 23 January 2015

Introduction

A distinctive geographic feature characteristic of the Colorado Rockies is the occurrence of high plateaus >2500-m elevation with complex vegetation mosaics of open grasslands, wet meadows, and tundra occurring between naturally fragmented stands of mature spruce and fir forests. Herbs, graminoids, forbs, and dwarf shrubs dominate the open expanses, while ecosystem dynamics are driven by fire; herbivory by elk, deer, and bison; and weather extremes. These areas also have an ~150-year-long history of Euro-American land use that includes hunting, mining, livestock grazing, logging, fire suppression, the introduction of invasive species, and motorized recreation (Vankat, 2013).

Documenting past vegetation and long-term trends using Holocene length ecological histories provides a means to understand the processes that influence ecosystem change, facilitates the identification of restoration targets, and informs management decisions (Jackson and Hobbs, 2009). Previous Holocene pollen studies from subalpine lake and bog sediments within the southern Rocky Mountains have documented changing geographic distributions of high elevation forests and treeline (Carrara, 2011; Fall, 1997; Feiler et al., 1997; Jiménez-Moreno and Anderson, 2013; Jiménez-Moreno et al., 2011; Reasoner and Jodry, 2000; Toney and Anderson, 2006). Less is known, however, about the long-term dynamics of grassland-meadow-forest distributions (Zier and Baker, 2006) particularly on high-elevation plateaus.

Here, we present multi-proxy data from the Holocene sediments of Bison Lake in northwest Colorado, located at 3255-m elevation in a complex vegetation setting with meadows, grasslands, tundra, and forests on the White River Plateau (WRP; Figure 1). Holocene hydroclimate variability is documented by calcite-$\delta^{18}O$ from sediment obtained at Bison Lake and nearby Yellow Lake (Anderson, 2011, 2012), which provides a rare opportunity to compare inferred landscape and ecosystem change with independently established hydroclimatic variations. Decade-to-century scale sampling resolution for the past ~13,000 years, using several proxy analyses, offers unusually detailed information about an ecosystem that few studies have targeted. The expected differences in ecosystem variations in

[1]U.S. Geological Survey, USA
[2]University of Utah, USA

Corresponding author:
Lesleigh Anderson, U.S. Geological Survey, Denver Federal Center Box 25046 MS-980, Denver, CO 80225, USA.
Email: land@usgs.gov

Figure 1. A panoramic view of Bison Lake from the northeast (left) to southwest (right).

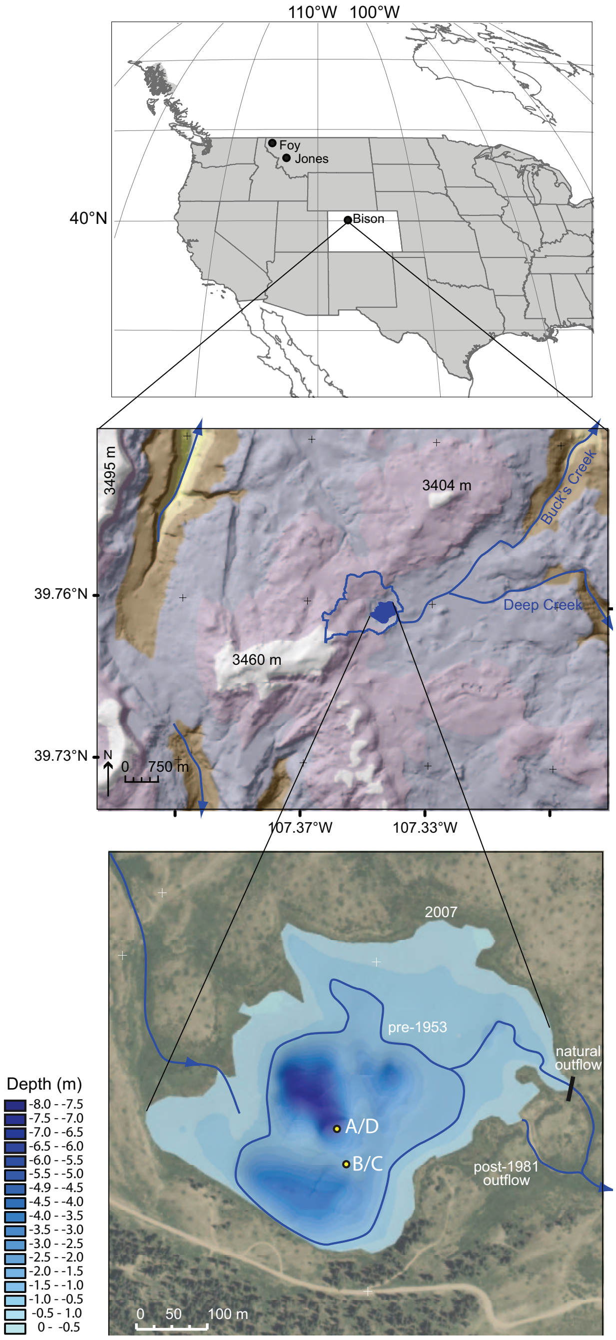

Figure 2. Locations of the White River Plateau (WRP) in northwest Colorado and the Bison Lake watershed on a shaded DEM, including bathymetry and the coring location for this study (A/D) and previous studies (B/C) on an aerial photograph. Records from Foy and Jones Lakes are discussed in the text.

physiographically complex mountains such as the Colorado Rockies (Redmond, 2003) necessitate landscape studies for specific ecological communities.

In addition to being one of the few multi-proxy studies in the southern Rocky Mountains, the basal age of the newly obtained Bison Lake record also provides the first minimum age for deglaciation of the WRP ice cap. The WRP ice cap was one of numerous high-elevation plateaus in western Colorado and Utah that were glaciated (Marchetti et al., 2011, and references therein). Terminal and lateral moraine evidence for WRP glaciation indicates a lower elevation limit of 2850 m that is presumed to reflect Pinedale (~35–12 ka) or older advances based on relative correlation with other dated moraine sequences (Kirkham et al., 1997; Meierding and Birkeland, 1980). The extent and decay of plateau ice caps provide unique paleoclimatic information because their sensitive response to changes in equilibrium-line altitude was so closely dependent on summit breadth and ice thickness (Manley, 1955; Rea et al., 1998).

Study area

The WRP is a domal uplift of Mississippian Leadville Limestone with nearly flat lying strata and abundant karst features (Maslyn and Davis, 1979). Bison Lake is located in Garfield County, and lies within The White River National Forest (39.764°N, 107.346°W, 3255 m, Figure 2), and is the headwater of Deep Creek, a tributary of the upper Colorado River. The lake has natural surface water inflow and outflow stream channels, a surface area of 0.6 km^2, and a watershed area of 1.7 km^2 with a maximum elevation of 3445 m (Figure 2). Mississippian Leadville Limestone is frequently exposed within the watershed (Tweto et al., 1978). The lake occupies a northeast-facing depression confined by glacial deposits, and its maximum depth is 8.8 m. Current lake levels are 1–2 m higher than early 20th-century levels since the outflow stream was heavily modified as part of impoundments, water diversions, and logging operations that occurred across the plateau following a severe bark beetle outbreak during the early 1940s (Supplemental Material, available online).

The Bison Lake SNOTEL station operated by the Natural Resource Conservation Service since 1986 (CO-07K12S) records a mean annual temperature of −1°C and mean annual precipitation of 91 cm with ~70% of the annual total represented by snow water equivalent (SWE). Total snowfall depths range from ~3 to 12 m, and while some areas are affected by wind scouring and remain snow free throughout the winters, others remain covered throughout the summer by wind-loaded snowdrifts. Average monthly diurnal temperature variations are above freezing between May and October and monthly averages are 12°C in July and August although frosts can occur in any month. Summer precipitation is spatially variable and related to both westerly frontal boundaries and convective thunderstorms associated with monsoon flow (Redmond, 2003).

The US Geological Survey (USGS) Southwest Regional Gap Analysis Program (GAP; USGS National Gap Analysis Program, 2005) classifies the land cover of the Bison Lake watershed as a matrix of open vegetation and forest types (Figure 3). This matrix is the result of the diversity of habitats created by differences in slope, aspect, exposure, and soils. Sedges (*Carex trigonous*) are found in shallow muddy areas along the Bison Lake shoreline, whereas dense stands of willow (*Salix*), with lesser amounts of

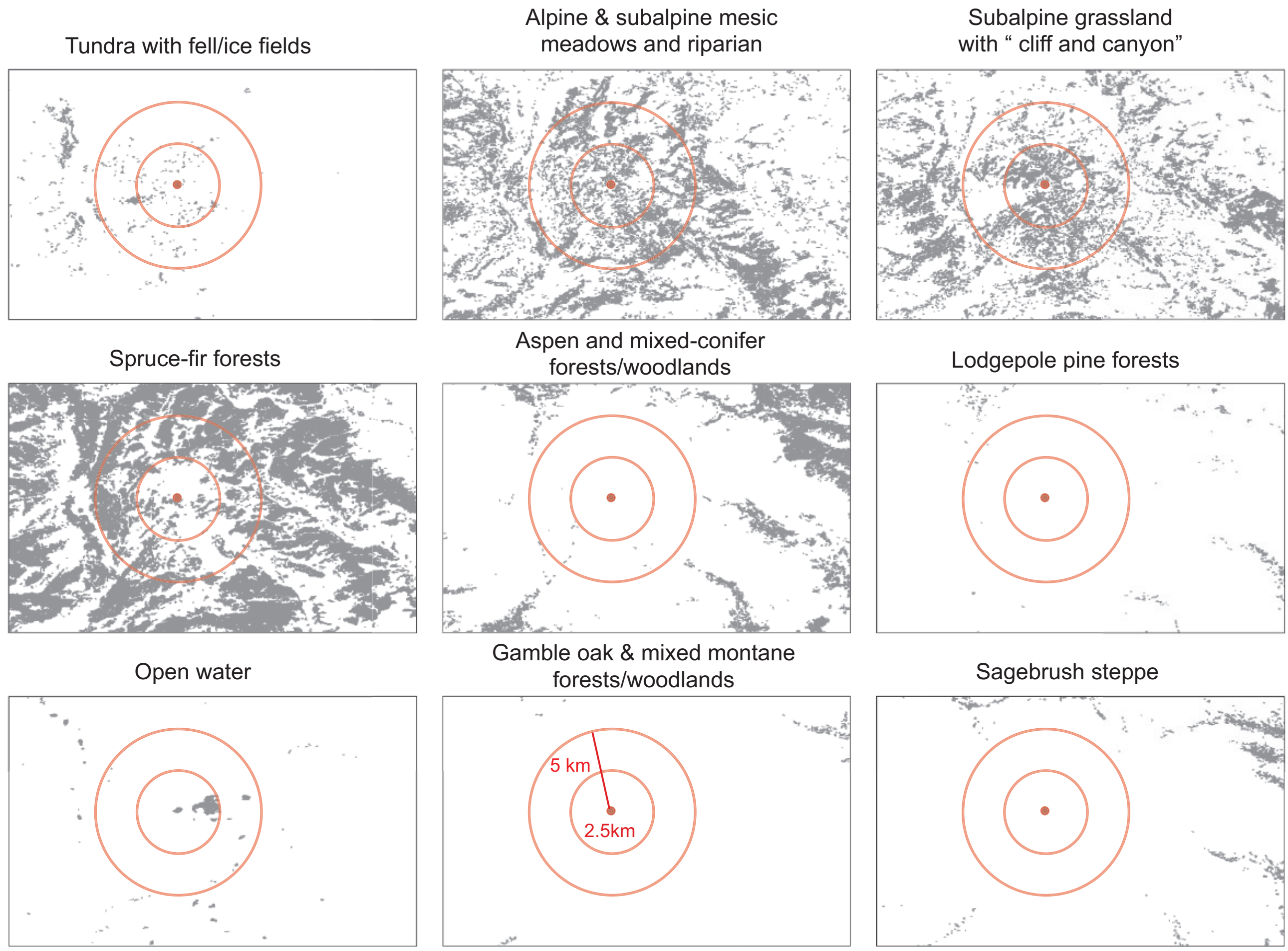

Figure 3. Land-cover types for the area on the WRP in relation to 2.5- and 5-km radius concentric areas around Bison Lake that illustrate the range of local pollen transport.

currant (*Ribes*), occupy rocky shorelines and inflow or outflow stream channels. Engelmann spruce (*Picea engelmannii*) cover the southern and western portions of the Bison Lake watershed, whereas the areas to the north and east of the lake are open subalpine grasslands, wet meadows, and rocky tundra related to slope, aspect, exposure, and soils.

Outside the watershed, the GAP land-cover maps indicate widespread occurrence of forest, woodlands, and steppe associations at surrounding lower elevations. Many of these associations include taxa that are prolific pollen producers, such as *Pinus, Quercus, Artemisia*, and Amaranthaceae. Although these taxa are not present in the Bison Lake watershed, high percentages of their pollen in the surface sample indicate that they contribute substantial amounts to the pollen spectra. Fir (*Abies*), limber pine (*Pinus flexilis*), Douglas fir (*Pseudotsuga menziesii*), and quaking aspen (*Populus tremuloides*) occur >5 km away between ~3000 and 2500 m. Sagebrush (*Artemisia*) and juniper (*Juniperus*) occur on dry, south-facing slopes below 2200 m (Figure 3).

Evidence suggests that prehistoric Native Americans commonly burned grasslands as a hunting practice (Stewart, 2002), and may have done so on the WRP. It is estimated that there were ~20,000 elk in the WRP herd ~1880 after settlement had begun by the first farmers, ranchers, and miners in or around 1863, but hunting rapidly thinned the herd thereafter (Boyd, 1970; Gulliford, 1983). By the late 1860s, Ute tribes had been confined to a small area along the WRP (Emmitt, 1954) and publication of accurate maps by the USGS's Hayden expedition in 1876 led to rapid population of the area by Euro-Americans. By 1879, a rush for lead and silver on the WRP led to the settlement of Carbonate township, located ~1.5 km south of Bison Lake. Located on exposed bedrock, most structures were tents built to house an estimated 2000–5000 prospectors during the peak of the rush. Mining was performed on a limited scale, mostly as prospect holes (Urquhart, 1967).

The Carbonate settlement was abandoned by 1886 as a result of failed mining claims and heavy snowfall during the winter of 1883–1884 (Urquhart, 1967). However, large herds of livestock were introduced so rapidly that by 1885, the plateau had already been characterized as overgrazed (Boyd, 1970). Following the establishment of public forest reserves in 1891, the USGS issued a report on WRP forest resources (Sudworth, 1900). Subsequent management was historically focused on timber, but cattle, horses, and sheep have had their summer range on the WRP continuously since the early 1900s.

Methods

The data presented here are from a 378-cm composite sediment core obtained in 2006 and 2010 from a securely anchored floating platform in 8.8 m water depth with a modified Livingstone corer (core A06). The uppermost 31 cm and undisturbed sediment–water interface was obtained using a customized polycarbonate tube fit with a piston (core D10). The composite core chronology A06–D10 is based on five AMS radiocarbon ages of terrestrial macrofossils and ^{210}Pb (Table 1). Radiocarbon ages were calibrated using CALIB 6.02 and 7.0 and are reported here as 'cal. yr BP' or as thousands of years ago, ka (Stuiver and Reimer, 1993). Measurements of ^{210}Pb were made on 1.0-cm slices to 30-cm depth. Water column parameters (temperature, pH, dissolved oxygen, and specific conductivity) were measured with calibrated Eureka or Hydrolab sondes in June and August of 2009 and July of 2006.

Table 1. Bison Lake core A06/D10 geochronological data.

Core depth (cm)	Material	Laboratory number[a]	Measured age (^{14}C yr BP)	Calibrated 1σ age ranges (relative area of distribution)	Median intercept of 1σ range (cal. yr BP)
0	Surface	–	–	–	−60
21	^{210}Pb horizon	–	–	–	89
58	Wood	WW6408	765 ± 35	673–711 (0.860); 717–723 (0.140)	698 ± 25
82	Wood	NSRL-17326	1545 ± 15	1399–1418 (0.392); 1466–1509 (0.608)	1454 ± 55
172	Conifer needle and plant fragments	NSRL-17327	3960 ± 20	4413–4439 (0.812); 4487–4498 (0.188)	4455 ± 43
210	Seed wing and plant fragments	NSRL-17328	5465 ± 20	6221–6231 (0.264); 6276–6294 (0.736)	6258 ± 37
372	Spruce needle	NSRL-19607	10,760 ± 40	12,677–12,721 (1.00)	12,685 ± 44
379	Bulk organic	NSRL-17329	14,435 ± 40	17,419–17,783 (1.00)	17,600 ± 182

AMS: accelerator mass spectrometry; USGS: US Geological Survey.
[a]NSRL laboratory numbers refer to the INSTAAR Laboratory for AMS Radiocarbon Preparation and Research and W.M. Keck Carbon Cycle AMS Facility. WW numbers refer to the USGS Eastern Geology and Paleoclimate Science Center ^{14}C Laboratory and either the NSF-Arizona AMS Facility or Lawrence Livermore CAMS Facility.

Whole core magnetic susceptibility was measured at 1-cm increments with a Bartington MS2 magnetic susceptibility system. Half core segments were scanned with a second-generation Cox Analytical ITRAX core scanner with Mo and Cr tubes at 1-cm resolution. The resulting output in elemental counts per minute was converted to centered natural log ratios (clr), a data treatment that eliminate effects related to physical sediment changes and corrects for the constant-sum issue of compositional measurements (Weltje and Tjallingii, 2008). As such, elemental XRF-clr results should be considered semiquantitative. In addition to x-radiographic images (Supplemental Material, available online), ITRAX scanning also produced measurements of incoherent and coherent x-ray scattering (inc/coh), a qualitative measure of organic matter content (e.g. Burnett et al., 2011).

Volumetric samples (1 cc) were taken at 1-cm increments for dry bulk density. Subsamples were taken every 2-cm to 220-cm depth, and every 15–20 cm thereafter, and pulverized to a fine powder for analysis of weight percentages of total carbon (TC) and total inorganic carbon (TIC) using a UIC, Inc. carbon dioxide coulometer (Englemann et al., 1985). Percent organic carbon was calculated as the difference between TC and TIC. Percent organic matter was calculated as 2.5 times the percent organic carbon, an approximation based on the molar fraction of carbon to hydrocarbons that make up lipids, carbohydrates, and proteins (Meyers and Teranes, 2001). Percent carbonate was calculated as TIC/0.12, where 0.12 is the molar fraction of carbon in $CaCO_3$. The accuracy and precision for both TC and TIC is 0.10%.

Pollen samples (1 cc) were taken at 4-cm increments for the upper 30 cm and at 8-cm increments thereafter and were processed following the methods described in Faegri et al. (1989). Known numbers of *Lycopodium* spores were added to each sample as an exotic tracer. For each sample, approximately 300 terrestrial pollen grains were identified to the lowest possible level of taxonomic classification at a magnification of 400×. Pollen counts were converted to percentages based on the sum of total terrestrial grains.

Macroscopic charcoal and macrofossil analyses were performed from contiguous 1-cm samples. Macroscopic charcoal >60 μm most likely represent local charcoal production during fires (Clark, 1988; Gardner and Whitlock, 2001; Whitlock and Millispaugh, 1996), and for each sample, charcoal counts were obtained for the >250- and >125-μm size fractions. Totals were converted to concentrations (particle #/cm^3) and accumulation rates (CHAR, #/cm^2/yr) were calculated using the age model.

Significant CHAR peaks were identified using CharAnalysis version 1.1 (Higuera et al., 2009; available online at http://sites.google.com/site/charanalysis). The charcoal time series was resampled using a weighted interpolation with a 40-year time step and then decomposed into low-frequency or background and peak components. Background CHAR variations were estimated within 500-year windows using a locally weighted regression robust to outliers (Lowess). Residual CHAR were calculated by subtracting background values from interpolated values to create the CHAR peak time series. Significant CHAR peaks (local fires) were identified by a locally determined threshold based on the 95th percentile of the noise distribution determined by a Gaussian mixture model and <5% probability of having originated from the same Poisson's distribution as the minimum charcoal count in the preceding 75 years (Higuera et al., 2010a). This last test is very sensitive to abrupt changes in sedimentation rate; such an abrupt change (from 30 to 15 yr/cm), associated with the linear age model, led to the software's exclusions of a prominent charcoal peak at ~AD 1250. However, because the raw charcoal count of the sample is comparable to all other significant peaks, it is still included in our analysis. Fire frequencies were smoothed over a 1000-year moving window, but results were found to be highly sensitive to the decomposition parameter choices, and therefore, we have chosen not to present them.

Results

Age model, sedimentology, and geochemistry

An age model for the composite core A06/D10 was determined by linear interpolation between the median intercepts from the 1σ range of the calibrated ^{14}C ages, the depth of the ^{210}Pb horizon, and the age of the surface (Figure 4). The Dotsero tephra occurs at 205-cm depth and would correspond with a linearly interpolated age of 6020 cal. yr BP. However, that age is significantly older than the age of 5180 cal. yr BP determined from another Bison Lake core obtained in 4.5-m water depth by bracketing AMS ages of terrestrial macrofossils (Anderson, 2011). It is also significantly older than the upper 1σ range of 5210 cal. yr BP from Dotsero lava encased wood measured by conventional radiocarbon methods (Giegengack, 1962), suggesting that the tephra may have undergone density settling (e.g. Anderson et al., 1984), and it is not included in the age model for core A06/D10. Surface sediment ages were determined from ^{210}Pb activities by the constant rate of supply (CRS) method (Appleby, 2001). Total activity declines from surface values of 42 pCi/g to background supported values of 1.58 pCi/g by 20-cm depth (Supplemental Material, available online). Ages were linearly interpolated from the lowermost age at 20-cm depth (AD 1860, −56 cal. yr BP) to the uppermost ^{14}C age at 58-cm depth (698 cal. yr BP). Holocene sedimentation rates range between 0.025 and 0.035 cm/yr with higher rates of ~0.15 cm/yr during the past 150 years.

Organic matter and inorganic carbonate compose >70% of the sediment dry mass, and this composition is reflected by low bulk

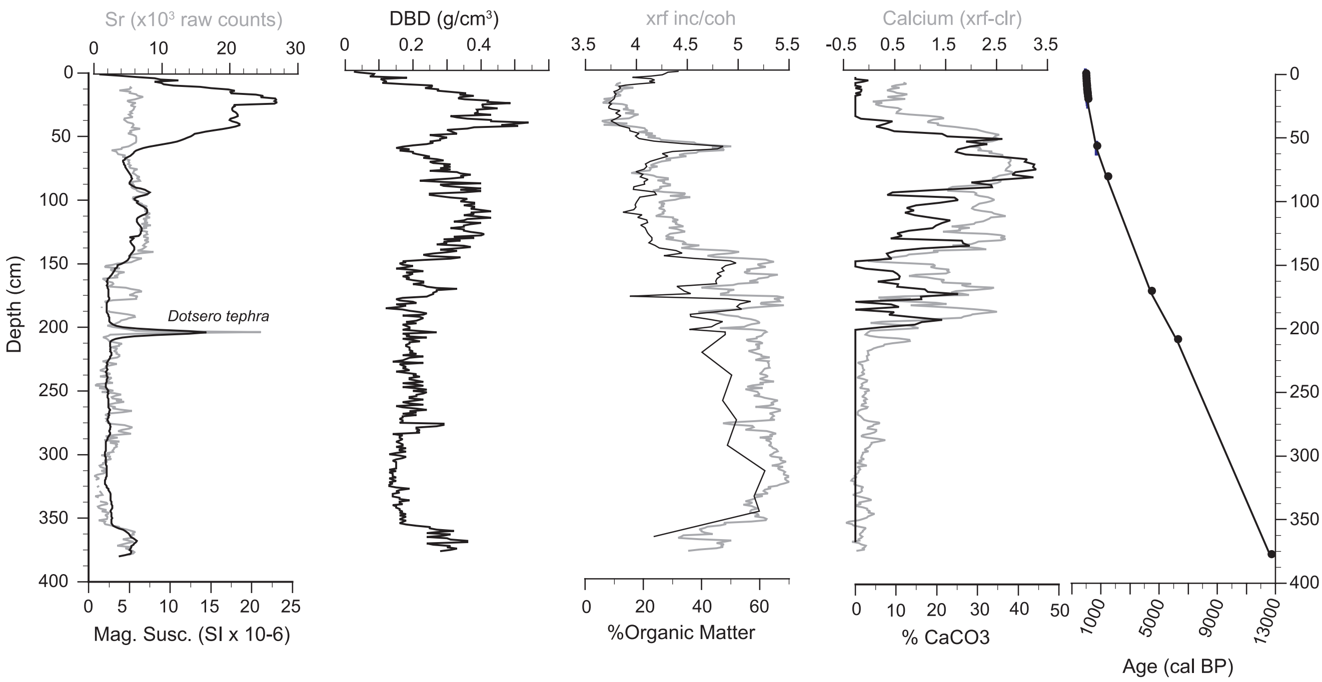

Figure 4. The physical properties of Bison Lake sediment (core A06/D10) on a vertical depth scale: a peak in magnetic susceptibility (black) with strontium (Sr) abundance (gray) indicates the presence of a tephra assumed to be Dotsero. Dry bulk density (DBD), percent organic matter, and calcite (black) are shown with incoherent and coherent x-ray scattering ratios (XRF inc/coh) and calcium abundances (gray) with ^{210}Pb and calibrated radiocarbon ages.

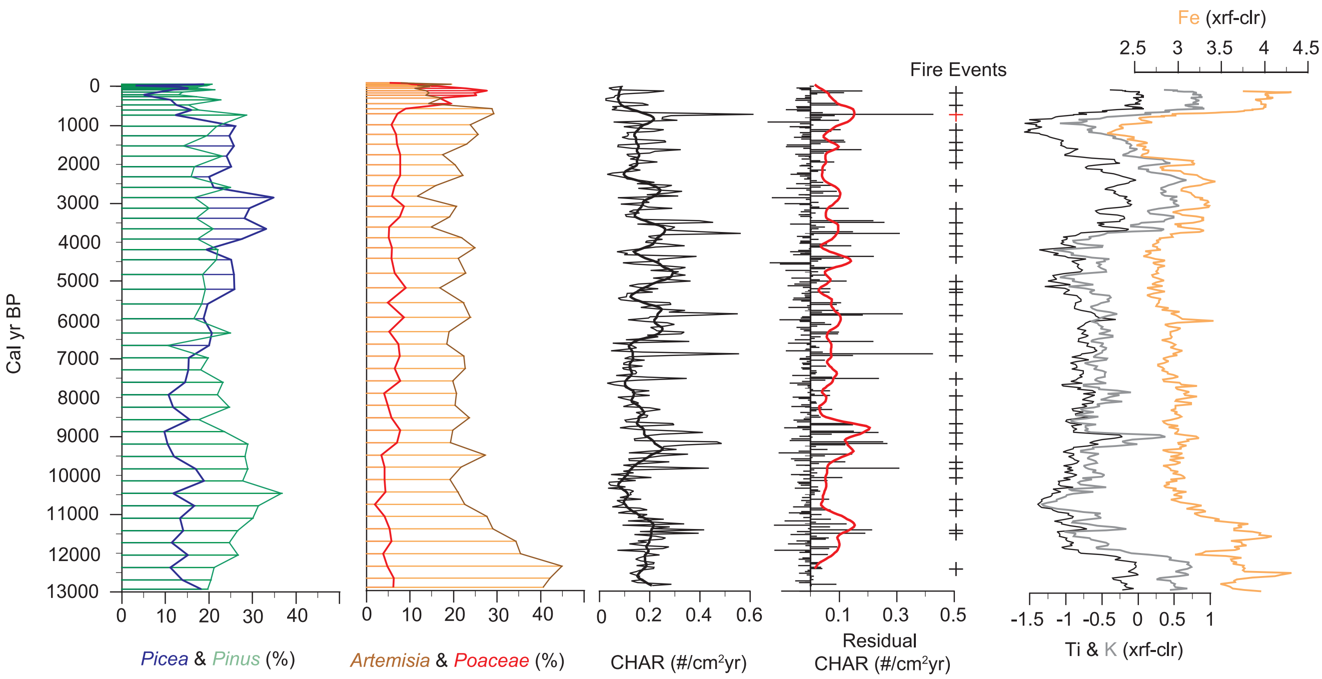

Figure 5. Major pollen taxa in Bison Lake, with CHAR, and detrital element abundances (Ti, K, and Fe) on a vertical calibrated age scale from 13,000 cal. yr BP to the present: *Picea* (blue), *Pinus* (green), Poaceae (red), and *Artemisia* (brown) pollen percentages; total CHAR and background (black); residual CHAR and peak threshold (red); local fire events (crosses, red peak at AD 1250 discussed in the text); and titanium (black), potassium (gray), and iron (rust) by XRF as centered natural log ratios (clr).

density values (0.05–0.45 g/cm³; Figure 4). Organic matter is in highest concentrations (~60%) between 300- and 350-cm depth, and values steadily decline up-core with the exception of peaks between 150- to 170-cm and 180- to 190-cm depth that correspond with an abundance of bryophyte macrofossils (*Drepanocladus)*. Bryophyte growth in deep water has been explained by low temperatures, extensive CO_2 supersaturation, and nutrient enrichment during summer stratification (Riis and Sand-Jensen, 1997). The prominent organic matter peak at 60-cm depth corresponds with a high charcoal peak centered at ~AD 1250.

Magnetic susceptibility values in the lower sections of the core are between 3 and 5 SI units with the exception of a peak at 205-cm depth that corresponds with a high-density band in x-ray images and raw XRF peaks in strontium (Sr) and iron (Fe) that identify the Dotsero tephra (Figures 4 and 5). Highest magnetic susceptibility values (>20 SI) occur in the upper 150 cm along with

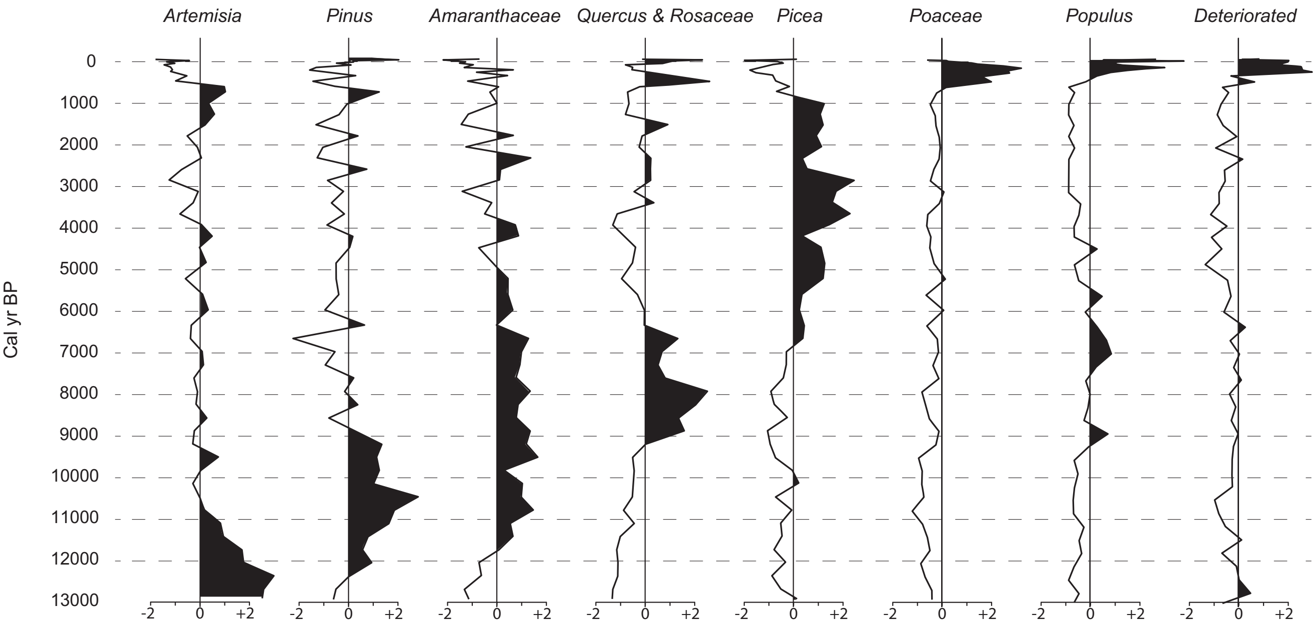

Figure 6. Standardized Bison Lake pollen percentages as z-scores for major taxa since deglaciation are presented for visualization purposes only. To standardize the percentage values across taxa, the long-term mean was subtracted from the value in a given sample and then divided by the standard deviation.

the highest density values (>0.4 g/cm^3) and lower organic carbon (<30%). The uppermost magnetic susceptibility variations strongly correspond to XRF changes in Fe, titanium (Ti), and potassium (K) that are derived from detrital mineral sources (Figure 5). Carbonate minerals were identified as endogenic calcite (i.e. $CaCO_3$ formed in situ) by x-ray diffraction and scanning electron microscopy and are absent in the lower half of the core. Occurrence begins at ~200-cm depth and amounts fluctuate between 0% and 20% before a sustained maximum of 40–45% between 35 and 75 cm (~2000–500 cal. yr BP). Thereafter, calcite concentrations rapidly declined to near zero up to the present day.

Pollen and charcoal

Forty-one terrestrial pollen types were identified (Supplemental Material, available online), and ~70% of the terrestrial pollen is composed of *Picea, Pinus, Artemisia*, and Poaceae (Figure 5). To better visualize the percentage data across pollen types with greatly differing mean values (Supplemental Material, available online), the stratigraphic profiles of important taxa are also presented in a standardized format in Figure 6. Lowermost sediments are dominated by *Artemisia*, with values between 30% and 45% that subsequently decline to a Holocene average of ~20% by 9000 cal. yr BP. Between 3000 and 800 cal. yr BP, *Artemisia* gradually rise to 28% and then decline after ~AD 1300 (Figure 6). At ~10,500 cal. yr BP, *Pinus* reached a maximum of 35% before declining to Holocene average values near 20% by ~9000 cal. yr BP. Amaranthaceae, *Quercus*, and Rosaceae rise between ~9000 and 6000 cal. yr BP. *Picea* gradually rise after ~9000 cal. yr BP and reach a Holocene maximum of 35% between 4000 and 3000 cal. yr BP. *Picea* decline dramatically after 1000 cal. yr BP, from ~26% to a Holocene minimum of 5% at ~AD 1750 (Figure 6). Poaceae percentages were near 15% throughout the record until ~AD 1200 after which they steadily increased to a Holocene maximum of 28% by ~AD 1800 soon followed by a rise in *Populus* and deteriorated pollen grains. Low pollen percentages of *Picea* during the 1700s and 1940s coincide with Engelmann spruce beetle outbreaks (Miller, 1970). Thereafter, Poaceae values declined to ~10% at the present day. *Abies*, although present on the WRP, was not observed at or near Bison Lake, and percentages are <5% throughout the record.

Total CHAR for the record ranged between 0 and 0.6 (#/cm^2/yr) and the statistical decomposition indicates 35 local fire events during the past ~13,000 years (Figure 5). CHAR software produces a median signal-to-noise index, and the value above which peaks were interpreted here is 2.83, which is well above the value expected for records without a peak signal (e.g. 0.15 for red noise). The most recent fire peak ~AD 1850 occurred prior to the start of fire observation (~1950) precluding comparisons between known fire events and the charcoal record for the site. Higuera et al. (2010b) determined that peaks most accurately reflected fires in a subalpine forest within 1.2–3.0 km of coring sites, and lower frequency variations in total CHAR background levels were found to correlate best within 6–51 km. Similarities between the subalpine ecosystem used in this study and that at Bison Lake suggest that these estimates may be applicable, and they are hereby referred to as ‘local fire events’ and ‘extra-local fire’, respectively.

Higher background levels representing extra-local fire occurred between 12,000–11,000 and 9500–8000 cal. yr BP. After ~6000 cal. yr BP, background levels regularly rose and fell in ~500 to 1000 years frequencies followed by slightly lower background levels between ~2000 and 1000 cal. yr BP. Higher background levels and a fire event at ~AD 1250 correspond with a spike in percent organic matter and corresponding decrease in calcite (Figure 7). Background CHAR declined during the transition into the ‘Little Ice Age’ (LIA), and peaks indicate local fire events during the late 1500s and early 1800s followed by the lowest Holocene background levels during the past ~100 years. To assess the significance of CHAR for selected time intervals, the accumulation data were binned and compared by t-test (Supplemental Material, available online). Middle and late Holocene means are statistically indistinguishable from each other but are significantly different from Medieval Climate Anomaly (MCA), LIA, and post-settlement periods.

Discussion

Timing of deglaciation at Bison Lake

Well-sorted, mineral-rich silt at the base of the core is low in organic matter, contains no calcite, has high density, and high in Fe, Ti, and K, all of which suggest allochthonous sedimentation

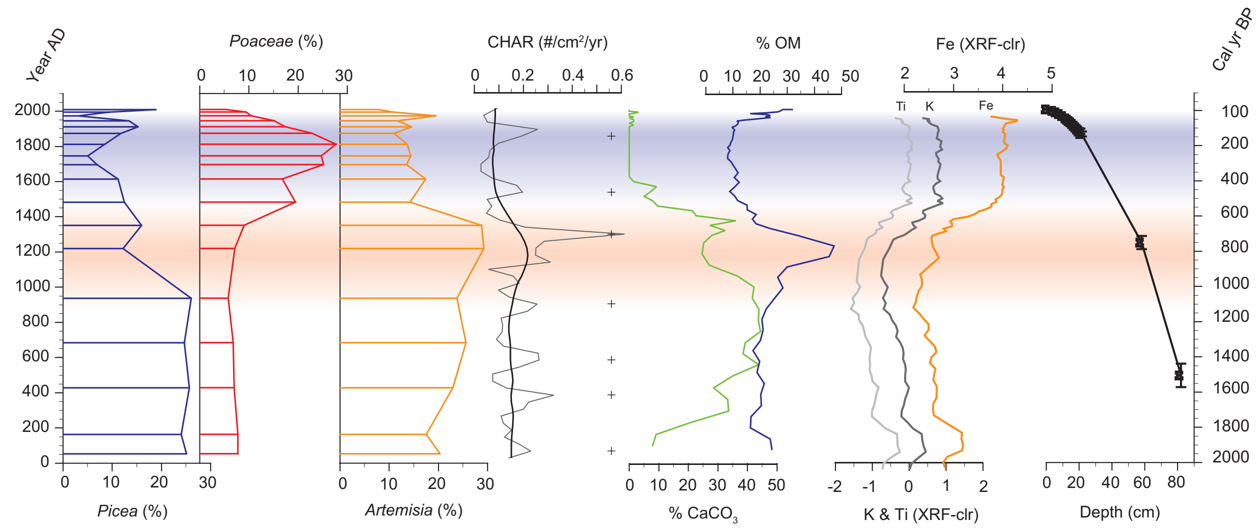

Figure 7. Expanded view of the past 2000 years with red shading over MCA and blue shading over LIA time periods: *Picea* (blue), Poaceae (red), and *Artemisia* (brown) pollen percentages; total CHAR (gray) and background (black); local fire events (crosses); percent organic matter (blue); and calcite (green), titanium (gray), potassium (black), and iron (rust) by XRF as centered natural log ratios (clr).

derived from a sparsely vegetated landscape following deglaciation of the plateau. Although the bulk organic fraction of the lowermost sediments provided an age of 17,600 cal. yr BP (14,435 ± 40 ^{14}C yr BP), the sample likely contained organic matter of aquatic origin that had incorporated old dissolved inorganic carbon (DIC). More reliable terrestrial material in the form of *Picea* sp. needle fragments were obtained 7 cm above the base of the core and provided an age of 12,700 cal. yr BP (10,760 ± 40 ^{14}C yr BP) that by linear extrapolation to the base of the core suggests a minimum confining age of deglaciation near ~13,000 cal. yr BP.

This age is contemporaneous with cirque glacier advances and down-slope displacement of upper treeline within the Colorado Rockies attributed to Younger Dryas (YD) cooling (Menounos and Reasoner, 1997; Reasoner and Jodry, 2000; Toney and Anderson, 2006). High percentages of *Artemisia* (45%) and relatively low *Picea* and *Pinus* percentages indicate that vegetation around Bison Lake was tundra or steppe consistent with a relatively cold and dry climate. The subsequent rapid increase in organic matter between 11,750 and 11,500 cal. yr BP marks the end of the YD cool period and the establishment of Holocene levels of within-lake biological productivity.

Hydroclimate

Holocene variations in hydroclimate for the WRP region, documented by the oxygen isotope ratios (δ^{18}O) of the endogenic calcite from Bison and nearby Yellow Lake, are described in detail by Anderson (2012). Differences in hydrology of the two lakes result in each lake-water's δ^{18}O reflecting different aspects of seasonal hydroclimate. Bison Lake values dominantly reflect the seasonal rain or snow balance of precipitation, whereas those of Yellow Lake reflect subsequent alteration by evaporation of light isotopes. Thus, Yellow Lake δ^{18}O values during the Holocene are generally 2–5‰ higher than Bison Lake (Figure 8). Because evaporation and snowfall effects occur during the summer and winter, respectively, larger δ^{18}O differences between the two lakes are likely the consequence of precipitation differences that occurred during summer and winter seasons.

During the early Holocene, higher δ^{18}O values and smaller differences (2‰) indicate greater rainfall proportions of the total precipitation amounts and lower overall effective moisture totals, consistent with generally lower alpine lake levels during that time (Shuman et al., 2009; Thompson et al., 1993; Toney and Anderson, 2006; Yuan et al., 2013). Bison Lake δ^{18}O declines after ~3500 cal. yr BP indicate multi-century periods of grater snowfall contributions to total precipitation amounts, consistent with Neoglacial cirque and rock glacier activity and greater ENSO activity (Anderson, 2011; Refsnider and Brugger, 2007).

Late Holocene Yellow-δ^{18}O values were either constant or higher, while snowfall amounts increased and thereby indicate correspondingly more water loss by summer evaporation. However, the combined Bison and Yellow-δ^{18}O data suggest that periods with colder and wetter winters during the late Holocene overcame the effects of warmer and drier growing seasons to drive positive long-term trends in net moisture balance indicated by other studies showing rising Rocky Mountain lake levels (e.g. Higuera et al., 2014; Minckley et al., 2012). Larger δ^{18}O differences characterize the periods of time when colder or wetter winters and warmer or drier summers occurred between ~2500 and 1500 cal. yr BP and during both the MCA and LIA.

Calcite abundance may also be related to hydroclimate. Calcite precipitation in Bison Lake is induced by photosynthesis of *Chara* macrophytes and other algae above the thermocline, where pH, temperature, and dissolved oxygen are high (9.5, ~15°C, and 11 mg/L, respectively). Surface sediments in locations above the thermocline are composed of >80% endogenic calcite, whereas calcite is absent below the thermocline with lower pH, temperature, and dissolved oxygen (~7.5, 7°C, <2 mg/L, respectively), and more dissolved CO_2 cause calcite dissolution. Thus, calcite variations in core A06/D10 could be related to changes in the strength and depth of stratification and/or rates of calcite production and dissolution related to biological productivity.

Seasonal overturn was not observed, but it seems possible that stratification would be highly variable across years with more or less spring runoff through the Holocene. Changes in biological productivity are understood from a commonly observed inverse relation between carbonate and organic matter (Dean, 1999; Wittkop et al., 2009). However, the highest calcite percentages of the Bison Lake record occurred during the MCA, and if this model were followed, the generally warm or dry growing seasons would have been expected to increase productivity (not decrease) and decrease calcite preservation (not increase). Alternatively, greater precipitation seasonality during the MCA could have led to thermal instability and more calcite preservation. It is also possible that marl bench development could have promoted greater calcite production by the gradual expansion of littoral areas of charophyte

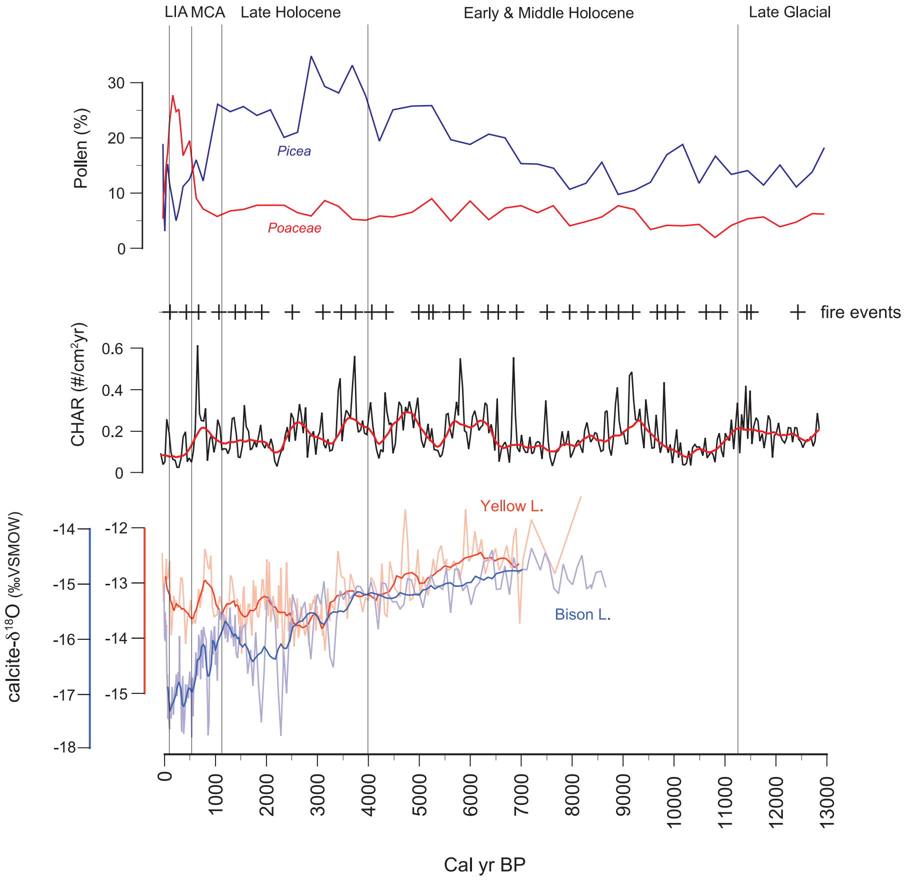

Figure 8. Bison and Yellow Lakes calcite-$\delta^{18}O$ records on a horizontal calibrated age scale shown with pollen and CHAR: *Picea* (blue), Poaceae (red) pollen percentages, total CHAR (black) and background (red), Bison (blue), and Yellow (red).

growth (Dustin et al., 1986). During the LIA, a Holocene maximum in terms of snowpack, shorter growing seasons would be consistent with more spring runoff, while lower calcite and organic matter production and higher detrital element abundances and higher magnetic susceptibility indicate reduced biological productivity and greater detrital sedimentation (Figure 7).

Fire

Bison Lake charcoal provides the first Holocene fire history for a subalpine plateau in northwest Colorado. Here, we interpret the Bison CHAR decomposition with an emphasis on the relationships between local fire events and extra-local trends with changes in local vegetation, watershed stability, and regional hydroclimate. Other studies have shown that regional networks of multiple macroscopic charcoal records are necessary to provide meaningful regional fire interpretations (e.g. Higuera et al., 2014; Marlon et al., 2012).

Since deglaciation and throughout the Holocene, local fire events at Bison Lake have been a regular occurrence (Figure 5). High background levels during the early and middle Holocene are consistent with more extra-local fire when higher Bison Lake $\delta^{18}O$ values suggest that winters were shorter and likely less severe, summer growing seasons were longer, and there was less overall effective moisture. Increased CHAR at ~9000 cal. yr BP corresponds with a significant peak in detrital elements, bulk density, and susceptibility that suggests more runoff from the watershed during a period of high fire severity (e.g. Dunnette et al., 2014).

A quiet extra-local fire period occurred between ~8000 and 6000 cal. yr BP, as *Picea* began to expand, in a stable watershed, and biological productivity within the lake was dominated by organic carbon sedimentation. Extra-local fire cycles resume at 500- to 1000-year intervals after ~6000 cal. yr BP when the $\delta^{18}O$ records indicate a steady trend toward more winter precipitation; *Picea* pollen reached ~20% and paleolimnologic proxies indicate a shift in the lake's nutrient and carbon budget to include carbonate, as well as abundant aquatic mosses and *Botryococcus* algae (Figures 4 and 8 and Supplemental Material, available online).

Extra-local fire and *Picea* declined after ~3000 cal. yr BP, likely driven by multi-decadal periods of greater snowfall indicated by abrupt declines in Bison Lake $\delta^{18}O$. Increases in extra-local fire between ~2500 and 1500 cal. yr BP and steady *Picea* pollen percentages (~25%) could reflect greater seasonality indicated by Bison and Yellow-$\delta^{18}O$, with colder or wetter winters possibly producing more fuel and warmer or drier (although likely shorter) growing seasons possibly driving more fire. High CHAR was sustained after ~900 cal. yr BP (AD 1100), with a peak at ~AD 1250 that may have been severe. The effects of this event on the landscape may have contributed to increased deposition of detrital elements soon thereafter (Figures 7 and 8). The ~AD 1250 fire peak corresponds with highly variable MCA hydroclimate characterized by extreme cold or wet winters and warm or dry drought-prone summers. Fire abruptly declined during the transition into the LIA after ~AD 1300 when *Picea* began a steep decline, and the hydroclimate proxies indicate a steep trend toward increasingly long, cold, and wet winters. Record low CHAR during the past century of Euro-American fire suppression is consistent with west-wide trends of fire suppression (Marlon et al., 2012).

Vegetation

Picea and Poaceae, the dominant taxa on the modern landscape, exhibit the most prominent pollen variations and are therefore the focus of our Holocene vegetation reconstruction (Figures 7 and 8). *Pinus* pollen is also prominent, and although lodgepole pine (*Pinus contorta*) is present on the WRP, it is neither near the lake today nor abundant in the local spruce forest. Therefore, modern *Pinus* pollen grains in Bison Lake sediments are likely transported to the site by wind from extra-local *Pinus contorta* trees and also from limber (*Pinus flexilis*, present but rare on the WRP), ponderosa (*Pinus ponderosa*), and pinyon pines (*Pinus edulis*), that are common at lower elevations (Fall, 1992b; Minckley et al., 2008). *Artemisia* pollen is also prominent and has been attributed to several species including the dominant steppe shrub *Artemisia tridentata*, the alpine species *Artemisia scolpulorum* (Fall, 1992a), and perhaps other common species in this genus (such as fringed sage (*Artemisia frigida*)). *Artemisia tridentata* does not occur in the immediate vicinity of the lake but dominates the sagebrush community between 2300 and 2900 m elevation on the WRP (Figure 3). Following the high percentages of *Artemisia* pollen that characterize the post-glacial environment at Bison Lake, values are near constant between 20% and 30% during the Holocene and likely reflect transport by wind from lower elevations. Similarly, *Populus*, Rosaceae, and *Quercus* pollen types varied between 0% and 10% throughout the record and probably originated from lower elevations.

The presence of *Picea* sp. needle fragments throughout the Bison Lake sediment record, including those that provide the basal age of 12,700 cal. yr BP, indicates that spruce forest was present from the earliest part of the record. Similarly, rapid post-glacial establishment of spruce has also been documented for the San Juan and Sangre de Cristo Mountains of southern Colorado (Carrara, 2011). There is close resemblance between early Holocene and present-day *Picea* and Poaceae pollen percentages (10–15% and 5–10%, respectively), suggesting a broadly similar open parkland during both periods.

A gradual increase in *Picea* in the early Holocene (as *Pinus* declined, *Artemisia* was constant, and Rosaceae and *Quercus* reached its highest levels) corresponds with higher $\delta^{18}O$ values that indicate less severe winters and longer growing seasons (Figures 6 and 8). During the late Holocene, between ~4000 and 2500 cal. yr BP, *Picea* reached peak abundance while the other major pollen types showed little change. This rise in spruce could represent a growth response to more moisture from winter snowfall indicated by lower $\delta^{18}O$ values. After ~2500 cal. yr BP, *Picea* declined slightly, recovered briefly, and then steadily declined during the past 1000 years. This decrease in spruce could represent mortality in response to shortened growing seasons. However, steady amounts of Poaceae and slight rises in *Artemisia* concurrent with the *Picea* decline suggest that it had little impact on the extent of open areas.

These relatively stable Holocene vegetation patterns changed significantly after ~AD 950 and the onset of the MCA (Figures 5 and 7). A sustained *Picea* decline between ~AD 950 and 1200 was paralleled by higher CHAR and $\delta^{18}O$, possibly indicating spruce mortality in response to drought and/or fire. There is little indication of significant assemblage change, however, as only *Artemisia* increased slightly during the initial *Picea* decline and Poaceae changed little. During the transition into the LIA between ~AD 1200 and 1500, expansion of herbaceous parkland appears to have been facilitated by greater snowfall and less fire as indicated by consistently low amounts of *Picea* and increased Poaceae, Asteraceae, and other herbs, in parallel with declines in CHAR and Bison Lake $\delta^{18}O$. A brief hiatus in the Poaceae rise and continued decline in *Picea* corresponds to fire episodes between AD 1550 and 1600. More open parkland appears to have developed over the next 200 years, until AD 1800 with little indication of fire. Poaceae is the dominant pollen within the assemblage at this time, and low Bison Lake $\delta^{18}O$ values indicate the coldest and snowiest winters of the Holocene. The results may suggest that while *Picea* suffered during LIA summers, not only most likely because they were shorter but also possibly because they were drier, Poaceae thrived, possibly due to greater thermal protection provided by greater snowfall.

Very low *Picea* pollen (5%) at ~AD 1750, near the lowest percentages of the Holocene, along with a sharp rise in *Populus*, Asteraceae, and other herbs and deteriorated pollen grains, corresponds precisely with well-documented spruce beetle outbreaks on the WRP in the early 1700s (Anderson et al., 2010; Miller, 1970; Veblen et al., 1994). However, the 100–200 years following the outbreak are not characterized by high fire. Instead, a subsequent rise in *Picea* pollen and decline in Poaceae suggests some closing of the parklands before fire episodes returned during the 1800s.

The multi-proxy Bison Lake record provides a new point of comparison with similar Holocene length studies that include $\delta^{18}O$-based reconstructions of hydroclimate from other locations within the Rocky Mountains that are based on comparisons between modern and paleo waters such as Foy and Jones Lakes in northwest Montana (Power et al., 2011; Shapley et al., 2009; Shuman et al., 2009). For instance, the Holocene $\delta^{18}O$ data from northwest Montana (Jones) and northwest Colorado (Bison, Yellow) indicate that a dry, rainfall-dominated early to middle Holocene, possibly related to enhanced monsoon activity, was also related to higher fire activity (Foy and Bison). The climate pattern presented by these interpretations is consistent with a growing body of evidence for negative Pacific Decadal Oscillation (PDO)-like (and Pacific North America Pattern (PNA)-like) zonal, northward displaced flow during early Holocene winters (e.g. Anderson, 2011; Liu et al., 2014). All of the records also indicate dramatic changes in hydroclimate, in terms of both seasonality and variability, after ~3500 cal. yr BP. These changes influenced vegetation, fire, or both in ways that are consistent with greater snowfall, shorter growing season length, reduced monsoon, and greater total effective moisture associated with enhanced ENSO and more positive PDO-like (PNA-like) patterns with greater ridge and trough structure and meridional flows over North America (e.g. Barron and Anderson, 2011).

Conclusion

The pollen, CHAR, and XRF record from Bison Lake clarifies both the timing of WRP deglaciation and the long-term dynamics of vegetation and fire for a northwest Colorado subalpine grassland ecosystem. The isotope data provide an independent measure of seasonal hydroclimatic variability, and their comparison broadly verifies a coarser pollen-based climate interpretation. However, pollen and CHAR interpretations of local to regional ecosystem dynamics in response to climate change are clearly strengthened by independent records of regional hydroclimate that include changes in seasonality. Overall, the combined proxies from Bison Lake provide consistent inferences that are summarized below.

Late glacial (13–10.5 ka)

There is no isotope data from Bison or Yellow Lakes for the period immediately following deglaciation of the WRP. A sparsely vegetated grassland was dominated by *Artemisia*, which declined by ~12,000 cal. yr BP as pine increased. Spruce was constantly present, and fire activity was infrequent.

Early and middle Holocene (10.5–4 ka)

The Bison Lake $\delta^{18}O$ record begins at ~10,000 cal. yr BP with the onset of calcite preservation, and high values reflect rainfall-dominated seasonality and less effective moisture. A drought period is likely responsible for high fire activity that denuded the landscape between ~9500 and 8500 cal. yr BP. For the next several millennia, the grassland–forest vegetation cover was largely stable with regular fire activity. A gradual decline in pine with a rise in spruce follows a gradual change to more snowfall, consistent with summer and winter insolation trends.

Late Holocene (4–1.2 ka)

The timing of negative Bison Lake $\delta^{18}O$ excursions, with the highest spruce percentages of the Holocene and lower fire activity after ~4000 cal. yr BP, suggests that the vegetation and fire changes were caused by a more snowfall-dominated precipitation balance. Therefore, a rise in detrital elements at this time appears to reflect more surface runoff from the watershed rather than reduced vegetation cover. Calcite became a greater component of lake sedimentation signifying that the hydroclimatic changes also affected lake stratification and/or biological productivity.

MCA and LIA to the present (1.2–0 ka)

The magnitudes of vegetation changes at Bison Lake that are documented during MCA-LIA periods were unprecedented in the Holocene reconstruction. Greater seasonal extremes characterize the climate variations. During the MCA, summers and winters were warmer or drier as spruce declined rapidly and fire activity increased. During the LIA, summers were still warmer or drier, but winters were colder or wetter as more open grasslands developed. Detrital elements indicate greater surface runoff, and calcite declines suggest strong lake stratification.

The pattern toward pollen of more open vegetation appears to deviate from that of nearby Antler Pond (Anderson et al., 2010). However, other sites in forested environments show a similar trend including nearby Dome Creek Meadow and Little Windy Hill Pond in southern Wyoming (Feiler et al., 1997; Minckley et al., 2012), Tiago Lake in north-central Colorado (Jiménez-Moreno et al., 2011), Kite Lake in central Colorado (Jiménez-Moreno and Anderson, 2013), and a small pond on Cottonwood Pass in central Colorado (Fall, 1997). Although the magnitude of change is larger at Bison Lake than in any of these other records, the timing of change is similar.

By extending through the period of Euro-American settlement, the combined proxy records provide a benchmark for distinguishing and assessing the relative effects of recent land-use change from those driven by natural climate variability. These results clearly show that the Bison Lake ecosystem was in response to unprecedented Holocene hydroclimatic change as it underwent additional pressure by fire suppression, hunting, and livestock grazing practices at the time of Euro-American settlement. This confluence of drivers appears to have changed the relative balance of the dominant land cover, but it did not lead to significant alterations of ecosystem composition. The Bison Lake record of climate and environmental change appears to illustrate significant ecosystem resilience in response to both low-frequency and short-term disturbance. Combined records of hydroclimate and ecosystem change provide a necessary long-term context for understanding the prospects of future Rocky Mountain forest health.

Acknowledgements

Jack McGeehan of the USGS Radiocarbon Laboratory and Chad Wolack of the University of Colorado Institute of Arctic and Alpine Research provided graphitization and AMS ^{14}C ages. Erik Brown of the University of Minnesota Duluth Large Lakes Observatory provided scanning XRF analyses and LaCore provided whole core magnetic susceptibility. Jessica Spencer of the University of Utah Records of Environmental Disturbance (RED) Lab provided pollen identification and charcoal analysis. Miriam Jones and Laura Strickland provided macrofossil identification, and Richard Pelltier provided GIS support. We appreciate comments by Dave Wahl and two anonymous reviewers that were helpful toward improving this article. Any use of trade, product, or firm names is for descriptive purposes only and does not imply endorsement by the US Government.

Declaration of conflicting interests

This draft manuscript is distributed solely for purposes of scientific peer review. Its content is deliberative and pre-decisional, so it must not be disclosed or released by reviewers. Because the manuscript has not yet been approved for publication by the USGS, it does not represent any official USGS finding or policy.

Funding

The U.S. Geological Survey (USGS) Climate and Land Use Research and Development Program provided the support for this research.

References

Anderson L (2011) Holocene record of precipitation seasonality from lake calcite $\delta^{18}O$ in the central Rocky Mountains, United States. *Geology* 39: 211–214. DOI: 210.1130/G31575.31571.

Anderson L (2012) Rocky Mountain Hydroclimate: Holocene variability and the role of insolation, ENSO, and the North American Monsoon. *Global and Planetary Change* 92–93: 198–208.

Anderson RS, Smith SJ, Lynch AM et al. (2010) The pollen record of 20th century spruce beetle (Dendroctonus rufipennis) outbreak in a Colorado subalpine forest, USA. *Forest Ecology and Management* 260: 448–455.

Anderson RY, Nuhfer EB and Dean WE (1984) Sinking of volcanic ash in uncompacted sediment in Williams Lake, Washington. *Science* 225: 505–508.

Appleby PG (2001) Chronostratigraphic techniques in recent sediments. In: Last WM and Smol JP (eds) *Tracking Environmental Change Using Lake Sediments: Basin Analysis, Coring, and Chronological Techniques*. Dordrecht: Kluwer Academic Publishers, pp. 171–203.

Barron JA and Anderson L (2011) Enhanced late Holocene ENSO/PDO expression along the margins of the eastern North Pacific. *Quaternary International* 235: 3–12.

Boyd RJ (1970) *Elk of the White River Plateau, Colorado* (Big Game Investigations Project W-38-R) (ed. LE Yeager). Technical Publication no. 25. Denver, CO: Colorado Division of Game, Fish and Parks.

Burnett AP, Soreghan MJ, Scholz CA et al. (2011) Tropical east African climate change and its relation to global climate: A record from Lake Tanganyika, tropical east Africa, over the past 90+kyr. *Palaeogeography, Palaeoclimatology, Palaeoecology* 303: 155–167.

Carrara PE (2011) *Deglacial and Postglacial Treeline Fluctuations in the Northern San Juan Mountains, Colorado*. US Geological Survey Professional Paper 1782. Denver, CO: U.S. Geological Survey.

Clark JS (1988) Particle motion and the theory of charcoal analysis: Source area, transport, deposition, and sampling. *Quaternary Research* 30: 67–80.

Dean WE (1999) The carbon cycle and biogeochemical changes in lake sediments. *Journal of Paleolimnology* 21: 375–393.

Dunnette PV, Higuera PE, McLauchlan KK et al. (2014) Biogeochemical impacts of wildfires over four millennia in a Rocky Mountain subalpine watershed. *New Phytologist* 203: 900–912. DOI: 10.111/nph.12828.

Dustin NM, Wilkinson BH and Owen RM (1986) Littlefield Lake, Michigan: Carbonate budget of Holocene sedimentation in a temperate-region lacustrine system. *Limnology and Oceanography* 31: 1301–1311.

Emmitt R (1954) *The Last War Trail: The Utes and the settlement of Colorado*. Boulder, CO: University Press of Colorado.

Englemann EE, Jackson LL, Norton DR et al. (1985) Determination of carbonate carbon in geological materials by coulometric titration. *Chemical Geology* 53: 125–128.

Faegri K, Kaland PE and Kzwinski K (1989) *Textbook of Pollen Analysis*. New York: Wiley.

Fall PL (1992a) Pollen accumulation in a montane region of Colorado, USA: A comparison of moss polsters, atmospheric traps, and natural basins. *Review of Palaeobotany and Palynology* 72: 169–197.

Fall PL (1992b) Spatial patterns of atmospheric pollen dispersal in the Colorado Rocky Mountains, USA. *Review of Palaeobotany and Palynology* 74: 293–313.

Fall PL (1997) Timberline fluctuations and late Quaternary paleoclimates in the Southern Rocky Mountains, Colorado. *GSA Bulletin* 109: 1306–1320.

Feiler EJ, Anderson RS and Koehler A (1997) Late Quaternary Paleoenvironments of the White River Plateau, Colorado, U.S.A. *Arctic and Alpine Research* 29: 53–62.

Gardner JJ and Whitlock C (2001) Charcoal accumulation following a recent fire in the Cascade Range, northwestern USA, and its relevance for fire-history studies. *The Holocene* 11: 541–549.

Giegengack RF (1962) *Recent volcanism near Dotsero, Colorado*. Unpublished Master's Thesis, Department of Geology, University of Colorado, 43 pp.

Gulliford A (1983) *Garfield County, Colorado: The First Hundred Years 1883–1983*. Glenwood Springs, CO: Grand River Museum Alliance.

Higuera PE, Briles CE and Whitlock C (2014) Fire-regime complacency and sensitivity to centennial through millennial-scale climate change in Rocky Mountain subalpine forests, Colorado, USA. *Journal of Ecology* 102: 1429–1441.

Higuera PE, Brubaker LB, Anderson PM et al. (2009) Vegetation mediated the impacts of postglacial climate change on fire regimes in the south-central Brooks Range, Alaska. *Ecological Monographs* 79: 201–219.

Higuera PE, Gavin DG, Bartlein PJ et al. (2010a) Peak detection in sediment-charcoal records: Impacts of alternative data analysis methods on fire-history interpretations. *International Journal of Wildland Fire* 19: 996–1014.

Higuera PE, Whitlock C and Gage JA (2010b) Linking tree-ring and sediment charcoal records to reconstruct fire occurrence and area burned in subalpine forests of Yellowstone National Park, USA. *The Holocene* 21: 327–341.

Jackson ST and Hobbs RJ (2009) Ecological restoration in the light of ecological history. *Science* 325: 567–569.

Jiménez-Moreno G and Anderson RS (2013) Pollen and macrofossil evidence of Late Pleistocene and Holocene treeline fluctuations from an alpine lake in Colorado, USA. *The Holocene* 23: 68–77.

Jiménez-Moreno G, Anderson RS, Atudorei V et al. (2011) A high-resolution record of climate, vegetation and fire in the mixed conifer forest of northern Colorado, USA. *GSA Bulletin* 123: 240–254.

Kirkham RM, Streufert RK and Cappa JA (1997) *Geologic Map of the Glenwood Springs Quadrangle, Garfield County, Colorado* (Map Series 31, scale 1:24,000). Denver, CO: Colorado Geological Survey.

Liu Z, Yoshimura K, Bowen GJ et al. (2014) Paired oxygen isotope records reveal modern North American atmospheric dynamics during the Holocene. *Nature Communications* 5: Article 3701. DOI: 10.1038/ncomms4701.

Manley G (1955) On the occurrence of ice-domes and permanently snow-covered summits. *Journal of Glaciology* 2: 453–456.

Marchetti DW, Harris MS, Bailey CM et al. (2011) Timing of glaciation and last glacial maximum paleoclimate estimates from the Fish Lake Plateau, Utah. *Quaternary Research* 75: 183–195.

Marlon JR, Bartlein PJ, Gavin DG et al. (2012) Long-term perspective on wildfires in the western USA. *Proceedings of the National Academy of Science* 109: E535–E543. DOI: 10.1073/pnas.1112839109.

Maslyn RM and Davis DG (1979) Karst development on the White River Plateau, Colorado. *National Speleological Society Bulletin* 41: 95–101.

Meierding TC and Birkeland PW (1980) Quaternary glaciation of Colorado. In: Kent HC and Porter KW (eds) *Colorado Geology*. Denver, CO: Rocky Mountain Association of Geologists, pp. 165–173.

Menounos B and Reasoner MA (1997) Evidence for cirque glaciation in the Colorado Front Range during the Younger Dryas chronozone. *Quaternary Research* 48: 38–47.

Meyers PA and Teranes JL (2001) Sediment organic matter. In: Last WM and Smol JP (eds) *Tracking Environmental Change Using Lakes Sediments*. Dordrecht: Springer, pp. 239–269.

Miller PC (1970) Age distributions of spruce and fir in beetle-killed forests on the White River Plateau, Colorado. *The American Midland Naturalist* 83: 206–212.

Minckley TA, Bartlein PJ, Whitlock C et al. (2008) Associations among modern pollen, vegetation, and climate in western North America. *Quaternary Science Reviews* 27: 1962–1991.

Minckley TA, Shriver RK and Shuman B (2012) Resilience and regime change in a southern Rocky Mountain ecosystem during the past 17,000 years. *Ecological Monographs* 21: 49–68.

Power MJ, Whitlock C and Bartlein PJ (2011) Postglacial fire, vegetation, and climate history across an elevational gradient in the Northern Rocky Mountains, USA and Canada. *Quaternary Science Reviews* 30: 2520–2533.

Rea BR, Whalley WB, Evans DJA et al. (1998) Plateau Icefields: Geomorphology and dynamics. *Quaternary Proceedings* 6: 35–54.

Reasoner MA and Jodry MA (2000) Rapid response of alpine timberline vegetation to the Younger Dryas climate oscillation in the Colorado Rocky Mountains, USA. *Geology* 28: 51–54.

Redmond KT (2003) Climate variability in the west: Complex spatial structure associated with topography, and observational issues. In: Lewis WM Jr (ed.) *Water and Climate in the Western United States*. Boulder, CO: University Press of Colorado, pp. 29–48.

Refsnider KA and Brugger KA (2007) Rock glaciers in central Colorado, U.S.A., as indicators of Holocene climate change. *Arctic, Antarctic and Alpine Research* 39: 127–136.

Riis T and Sand-Jensen K (1997) Growth reconstruction and photosynthesis of aquatic mosses: Influence of light, temperature and carbon dioxide at depth. *Journal of Ecology* 85: 359–372.

Shapley MD, Ito E and Donovan JJ (2009) Late glacial and Holocene hydroclimate inferred from a groundwater flow-through lake, Northern Rocky Mountains, U.S.A. *The Holocene* 19: 523–535.

Shuman B, Henderson AK, Colman SM et al. (2009) Holocene lake-level trends in the Rocky Mountains, U.S.A. *Quaternary Science Reviews* 28: 1861–1879.

Stewart OC (2002) *Forgotten Fires, Native Americans and the transient wilderness*. Norman, OK: University of Oklahoma Press.

Stuiver M and Reimer PJ (1993) Extended ^{14}C data base and revised Calib 3.0 ^{14}C age calibration program. *Radiocarbon* 35: 215–230.

Sudworth GB (1900) *The White River Plateau and Battlement Mesa Forest Reserves*. U.S. Geological Survey 20th annual report. Denver, CO: US Geological Survey.

Thompson RS, Whitlock C, Bartlein PJ et al. (1993) Climatic changes in the Western United States since 18,000 yr B.P. In: Wright HE Jr, Kutzbach JE, Webb T III, et al. (eds) *Global Climates Since the Last Glacial Maximum*. Minneapolis, MN: University of Minnesota Press, pp. 468–513.

Toney JL and Anderson RS (2006) A postglacial palaeoecological record from the San Juan Mountains of Colorado USA: Fire, climate and vegetation history. *The Holocene* 16: 505–517.

Tweto O, Moench RH and Reed JC (1978) *Geologic Map of the Leadville 1° x 2° Quadrangle, Northwest Colorado* (US Geological Survey Miscellaneous Investigations Map I-999, scale 1:250,000). Denver, CO: US Geological Survey.

Urquhart LN (1967) *Cold Snows of Carbonate*. Denver, CO: Golden Bell Press.

USGS National Gap Analysis Program (2005) *Southwest Regional GAP Analysis Project – Land Cover Descriptions*. Logan, UT: RS/GIS Laboratory, College of Natural Resources, Utah State University.

Vankat JL (2013) *Subalpine-Montane Grassland. Vegetation Dynamics on the Mountains and Plateaus of the American Southwest*. Dordrecht: Springer, 461 pp.

Veblen TT, Hadley KS, Nel EJ et al. (1994) Disturbance regime and disturbance interactions in a Rocky Mountain subalpine forest. *Journal of Ecology* 82: 125–135.

Weltje GJ and Tjallingii R (2008) Calibration of XRF core scanners for quantitative geochemical logging of sediment cores: Theory and application. *Earth and Planetary Science Letters* 274: 423–438.

Whitlock C and Millispaugh SH (1996) Testing the assumptions of fire-history studies: An examination of modern charcoal accumulation in Yellowstone National Park, USA. *The Holocene* 6: 7–15.

Wittkop CA, Teranes JL, Dean WE et al. (2009) A lacustrine carbonate record of Holocene seasonality and climate. *Geology* 37: 695–698.

Yuan F, Koran MR and Valdez A (2013) Late glacial and Holocene records of climatic change in the southern Rocky Mountains from sediments in San Luis Lake, Colorado, USA. *Palaeogeography, Palaeoclimatology, Palaeoecology* 392: 146–160.

Zier JL and Baker WL (2006) A century of vegetation change in the San Juan Mountains, Colorado: An analysis using repeat photography. *Forest Ecology and Management* 228: 251–262.